# Structure of superheavy hydrogen $^{7}$H

M. Caamaño[1,*], T. Roger[2,**], A. M. Moro[3], G. F. Grinyer[4], J. Pancin[2], S. Bagchi[5], S. Sambi[6], J. Gibelin[7], N. Itagaki[8], B. Fernández–Domínguez[1], J. Benlliure[1], D. Cortina-Gil[1], F. Farget[2], B. Jacquot[2], D. Pérez Loureiro[2], B. Pietras[1], R. Raabe[6], D. Ramos[1], C. Rodríguez–Tajes[2], H. Savajols[2], and M. Vandebrouck[9]

[1]IGFAE – U. de Santiago de Compostela, E–15782 Santiago de Compostela, Spain.
[2]GANIL, CEA/DSM – CNRS/IN2P3, BP 55027, F–14076 Caen Cedex 5, France.
[3]U. de Sevilla, E–41080 Sevilla, Spain.
[4]Department of Physics, University of Regina, Regina, SK S4S 0A2, Canada.
[5]KVI–CART, U. of Groningen, NL–9747 AA, Groningen, The Netherlands.
[6]Instituut voor Kernen Stralingsfysica, KU Leuven, B–3001 Leuven, Belgium.
[7]LPC de Caen, U. de Caen Basse–Normandie – ENSICAEN – CNRS/IN2P3, F–14050 Caen Cedex, France.
[8]Yukawa Institute for Theoretical Physics, Kyoto University, 6068502 Kyoto, Japan.
[9]IPN Orsay, U. Paris Sud, IN2P3 – CNRS, F–91406 Orsay Cedex, France.

**Abstract.** The properties of nuclei with extreme neutron–to–proton ratios reveal the limitations of state-of-the-art nuclear models and are key to understand nuclear forces. $^{7}$H, with six neutrons and a single proton, is the nuclear system with the most unbalanced neutron–to–proton ratio ever known, but its sheer existence and properties are still a challenge for experimental efforts and theoretical models. We report here the first measurement of the basic characteristics and structure of the ground state of $^{7}$H; they depict a system with a triton core surrounded by an extended four-neutron halo, built by neutron pairing, that decays through a unique four–neutron emission with a relatively long half-life. These properties are a prime example of new phenomena occurring in almost pure-neutron nuclear matter, beyond the binding limits of the nuclear landscape, that are yet to be described within our current models.

## 1 Introduction

Our understanding of how nucleons interact in order to build up nuclei with specific underlying structures can be tested and improved at the extremes of the nuclear chart. A particularly distinct limit of the nuclear landscape is given by the proton and neutron drip-lines: beyond these borders, nuclei are unstable against proton and neutron emission, and thus they are formed in the continuum, into relatively loose resonance states with very short half-lives but well-defined structures [1]. These systems are good examples of instances where the nuclear interaction begins to fail binding up nucleons into nuclei. In this respect, light nuclei are very convenient to reach systems beyond the drip-lines: adding or subtracting a few nucleons is enough to reach the continuum. This is particularly true in the case of hydrogen isotopes: the addition of neutrons to stable hydrogen isotopes allowed to reach, so far, four resonances in the continuum – $^{4}$H, $^{5}$H, $^{6}$H, and $^{7}$H –, making it the longest isotopic chain outside the limits of the nuclear chart. In addition, the low proton content renders these isotopes as a good test field for almost pure neutron-neutron interaction. Finally, if we define exotic nuclei attending at their neutron-to-proton ratio, the last isotope of the chain, the $^{7}$H resonance, can be identified as the most exotic nuclear system studied in the laboratory.

The properties of $^{7}$H are not restricted to its exotic characterisation. The few theoretical attempts to describe the system predict $^{7}$H as a low-lying resonance below 3 MeV over the $^{3}\mathrm{H} + 4\mathrm{n}$ subsystem mass [7] due to the cohesive effect of the neutron pairing. Such a low mass would make it possible to decay directly to $^{3}$H through a unique simultaneous emission of four neutrons associated with a narrow resonance width [8]. Its structure may also display a distinctive di-neutron condensate halo around a $^{3}$H core, which would extend up to a 6-fm radius [2]. With these numbers, the density and neutron-to-proton ratio of the $^{7}$H system would be akin to those expected to be found in the inner crust of neutron stars [3]. These out-of-core neutrons are expected to sit on the $p_{3/2}$ shell, leaving the ground state of $^{7}$H with a $1/2^{+}$ spin and parity.

In general, the experimental study of hydrogen resonances is a challenging one. Their production cross sections are small, their short half-lives prevent a direct measurement, and their multi-particle decays complicate the reconstruction of the reactions. In the case of $^{7}$H, we find only three experiments with evidences of its formation [4–6]. The results in all of them share similar features: an increase in the production cross section, namely a peak, was found around a certain resonance mass, but low statistics

*e-mail: manuel.fresco@usc.es
**e-mail: thomas.roger@ganil.fr

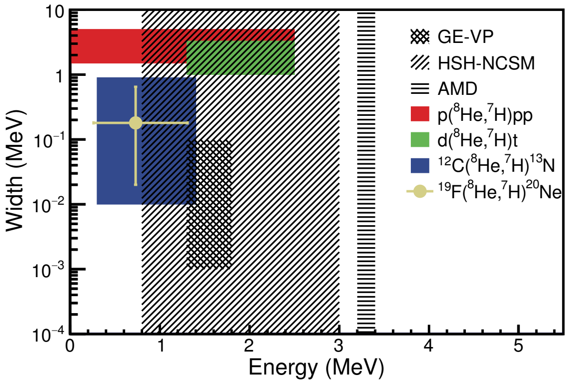


**Figure 1.** Summary of theoretical and experimental results on $^7$H. Hatched areas correspond to predicted width and mass values from Gaussian emission off of a Volkov Potential (double hatching, GE-VP) [8], Hyper-Spherical Harmonics with No-Core Shell Model (tilted hatching, HSH-NCSM) [7], and Anti-symmetrized Molecular Dynamics (horizontal hatching, AMD) [2]. The colour regions correspond to experimental results from p ($^8$He , $^7$H) pp knockout (red) [4], d ($^8$He , $^7$H) t (green) [5], and $^{12}$C ($^8$He , $^7$H)$^{13}$N (blue) [6]. The gold point corresponds to the present experiment.

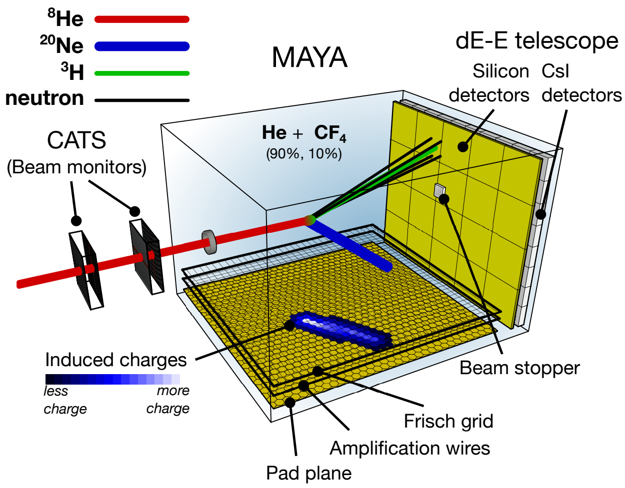


**Figure 2.** The $^7$H resonance was produced and measured within the MAYA active target. A $^8$He beam projectile is tracked and monitored with the CATS detectors before entering MAYA and colliding with a $^{19}$F atom contained in the He + $CF_4$ filling gas, producing a $^{20}$Ne nucleus and a $^7$H resonance that decays into a $^3$H nucleus and four neutrons. The $^3$H nucleus is stopped and identified in the dE–E telescope, while the trajectory of the $^{20}$Ne nucleus is projected onto the segmented pad plane and recorded.

and a poor resolution limit the definition of the parameters of the resonance. Figure 1 shows a summary of the theoretical and experimental results on the $^7$H width and mass we can find in the literature.

Two main remaining issues can be identified in the study of $^7$H: An accurate determination of its parameters, and an independent confirmation of its detection by using observables other than a peak on the production. In this paper we present a new, improved measurement of the resonance and its parameters, as well as the confirmation of its identification through the measurement of the differential cross section. This observable also allow us to assign the spin and parity of the ground state of $^7$H.

## 2 Experimental set-up

The experiment was performed at GANIL (France), where the Spiral facilities delivered a $10^4$ pps, 15.4 AMeV $^8$He beam, which was directed towards the experimental setup, composed of the CATS beam monitors [9] and the MAYA active target [10]. The MAYA device is based on the detection principles of a gas Time-Charge Projection Chamber, with the filling gas acting as reaction target. In this case, MAYA was filled with a gas mixture of helium and $CF_4$, with equivalent thickness of $4 \times 10^{19}$ and $10^{19}$ atoms/cm$^2$ for $^{12}$C and $^{19}$F, respectively. In a typical proton transfer reaction, a $^8$He projectile hits a $^{19}$F nucleus and transfers a proton, producing a $^{20}$Ne target-like and, possibly, a $^7$H resonance. In these events, the $^7$H decays in a very short time, producing a $^3$H nucleus and four neutrons. The scattered $^3$H is detected in a dE-E telescope at the end side of MAYA, where it is identified and its energy measured. The target-like recoil $^{20}$Ne is stopped inside the filling gas, and the electrons from the ionisation produced along its trajectory are directed towards a segmented pad plane in order to produce a projected image of its path. The drift time measurement completes the three-dimensional characterisation of this trajectory. Light particles, with atomic numbers below Z = 4, do not ionise the gas enough to induce signals in the segmented cathode. Figure 2 shows a schematic explanation of the process. An equivalent event might take place should the $^8$He hit a $^{12}$C nucleus instead a $^{19}$F.

Events suspected of having undergone $^{19}$F ($^8$He , $^7$H) $^{20}$Ne or $^{12}$C ($^8$He , $^7$H) $^{13}$N reactions are selected among those with $^3$H as a single beam-like recoil and a single trajectory recorded in the pad plane. This selection rules out multi-particle channels and reactions with the helium nuclei in the gas. Ideally, the measured range and angle of the target-like trajectory are correlated through the kinematics of the reaction, provided that a binary reaction has taken place. In our case, the uncertainty on the range measurement prevents from a direct identification of the kinematic lines. Figure 3 shows the range–angle correlation for the events selected as described previously. Figure 4 shows the range distribution of events with angles between 45° and 54°. The excess of counts around 60 mm cannot be explained by any reaction channel except the one-proton transfer between $^{19}$F and $^8$He, and it is thus assigned to the production of the $^7$H resonance. In order to extract the width and mass of the resonance, an exhaustive simulation of the kinematics of all the reaction channels involved, including phase-space distributions, folded with experimental uncertainties and efficiencies was used to find the resonance parameter that best fitted the measured data. The fitting process was iterated for different angular regions and data subsets in order to test the stability of the results and determine their uncertainties.

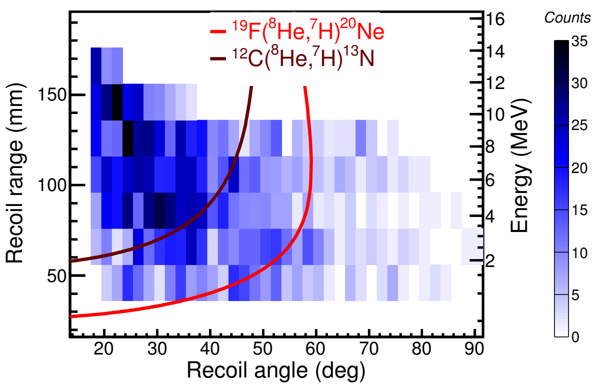


**Figure 3.** The color scale shows the measured events of the target–like recoil in coincidence with the detection of a $^3$H as a beam–like scattered product on the dE–E telescope. Solid red/dark red lines correspond to the kinematics of $^{19}$F ($^8$He , $^7$H) $^{20}$Ne and $^{12}$C ($^8$He , $^7$H) $^{13}$N, respectively.

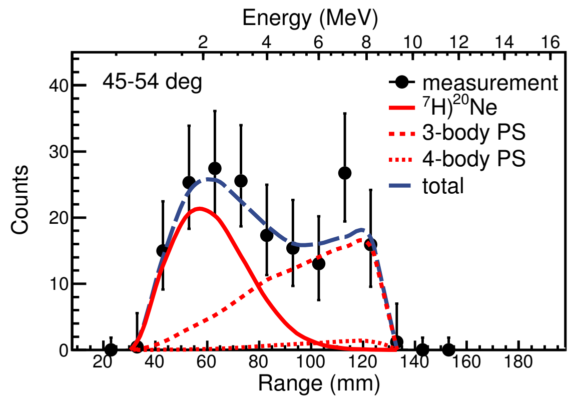


**Figure 4.** The $^7$H resonance peak is observed in the range (lower axis)/energy (upper axis) distribution of target–like recoils between 45° and 54°. The histogram data is in coincidence with the identification of a $^3$H beam–like scattered particle, and corrected by geometrical efficiency. Simulated distributions of the $^7$H resonance (solid red line), and 3–body and 4–body phase–space (PS) (dashed and short–dashed red lines) are fitted to determine the characteristics of the resonance.

## 3 Results

The optimization of the resonance parameters in the simulation, resulted in a resonance width of $\Gamma_{7H} = 0.18^{+0.47}_{-0.16}$ MeV and a mass of $E_{7H} = 0.73^{+0.58}_{-0.47}$ MeV over the mass of the $^3$H + 4n subsystem. This result confirms $^7$H as a low-lying resonance with a relatively long half-life of $\sim 3\times10^{-21}$ s. For reference, $^{4,5,6}$H resonances have masses above 1.5 MeV and half-lives shorter than $0.7 \times 10^{-21}$ s. The fact that $^7$H is the least unstable of them all, also suggests a simultaneous four-neutron emission as its decay channel, without populating intermediate resonances. Such a multi-particle decay is coherent with its narrow width [8]. The comparison with previous results shows a good agreement with the previous MAYA experiment [6] while, in general, theory seemed to overestimate the resonance mass.

The observation of an accumulation of events around a certain range or, equivalently, energy can be a straightforward consequence of the formation of a well-defined system. However, the opposite might not be true: a peak may be produced by other means, from statistical fluctuations (in particular when dealing with low statistics) to artefacts from unknown effects in the measurements or even contamination from other sources and reaction channels. In this work, we seek to confirm the formation of $^7$H with another observable: the differential cross section. From the fitting of the detailed simulation to the experimental data we obtain the number of events where the $^7$H was produced, already corrected by the detection efficiency and acceptance, for different regions in the centre-of-mass angle. These numbers are translated to cross section with the ratio to the number of target atoms in the gas and the number of incident beam particles, measured with the CATS monitors. The resulting cross section for the $^{19}$F ($^8$He , $^7$H) $^{20}$Ne is displayed in Fig. 5.

As we can see in Fig. 5, the measured cross section has an oscillating pattern, with clear maxima and minima, along the centre of mass angle. The figure also displays different calculations, performed with the coupled reaction channels, DWBA code FRESCO [11], assuming different configurations for the final state in both products, the $^7$H resonance and the target-like $^{20}$Ne. We have also included the description of the ground state of the $^7$H given by the Anti-symmetrized Molecular Dynamics code [2], which we found the most accurate about the position of the minima. The measured data is best reproduced by a proton transfer producing $^{20}$Ne in its $0^+$ ground state and a $^7$H in a $1/2^+$ state. The low mass measured for $^7$H and the assigned $1/2^+$ spin and parity are coherent with the detection of its ground state. The measured cross section is an independent confirmation that we are indeed observing the formation of the $^7$H resonance as a nuclear system with well-defined quantum properties.

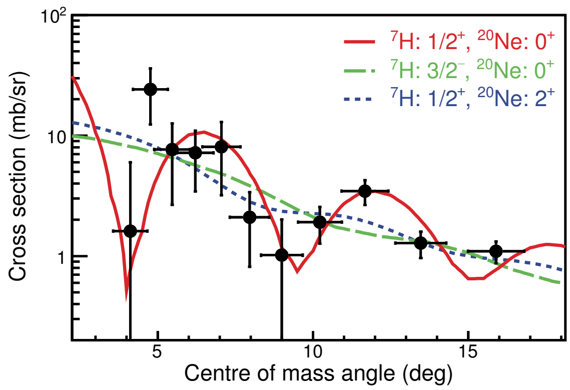


**Figure 5.** Differential cross section of the $^{19}$F ($^8$He , $^7$H) $^{20}$Ne transfer channel. The experimental data set (black dots) is well reproduced by a DWBA calculation of the transfer reaction producing a $^7$H resonance in a $1/2^+$ level and a $^{20}$Ne in its $0^+$ ground state (red line). Other plausible scenarios (green and blue lines) do not follow the measured data.

## 4 Conclusions and perspectives

In this work, we have measured the production of the $^{7}$H resonance through one-proton transfer reactions between a $^{8}$He beam and $^{19}$F and $^{12}$C nuclei within a composite He + $CF_4$ gas target with the MAYA active target. Although, for brevity, we present here only the analysis of the $^{19}$F channel. Our results confirm the existence of $^{7}$H as a low-lying, long-lived resonance. This confirmation is backed up by the measurement of the differential cross section, which allows us to assign a $1/2^{+}$ spin and parity to the $^{7}$H ground state.

These results contribute to forming a general understanding of nuclear structure outside the binding limits of the nuclear chart. In the case of $^{7}$H, the neutron pairing is able to build an extended halo around the $^{3}$H, and it is strong enough to make $^{7}$H the least unstable of the hydrogen resonance chain in the continuum, despite being the heaviest and most exotic of them all. Theory gives us a hint of the large size of this halo [2], which can also be pictured as a dilute boson condensate, with neutron pairs acting as neutral bosons. The behaviour of neutrons and neutron pairing in such environment is relevant for the study of nuclear structure [12], but it is also important for the understanding of dilute nuclear matter in astrophysical scenarios, such as neutron stars, and the formation of even more exotic nuclear systems [13].

## References

[1] P. G. Hansen, Nature **328**, 476 (1987).
[2] S. Aoyama, N. Itagaki, Phys. Rev. C **80**, 021304(R) (2009).
[3] N. Chamel, P. Haensel, Living Rev. Relativity **11**, 10 (2008).
[4] A. A. Korsheninnikov, E. Yu. Nikolskii, E. A. Kuzmin *et al.*, Phys. Rev. Lett. **90**, 082501 (2003).
[5] S. Fortier, E. Tryggestad, E. Rich *et al.*, AIP Conf. Proc. **912**, 3 (2007).
[6] M. Caamaño, D. Cortina-Gil, W. Mittig *et al.*, Phys. Rev. Lett. **99**, 062502 (2007).
[7] N. K. Timofeyuk, Phys. Rev. C **69**, 034336 (2004).
[8] M. S. Golovkov, L. V. Grigorenko, A. S. Fomichev *et al.*, Phys. Lett. B **588**, 163 (2004).
[9] S. Ottini-Hustache, C. Mazur, F. Auger *et al.*, Nucl. Instr. and Meth. A **43**, 475 (1999).
[10] C. E. Demonchy, M. Caamaño, H. Wang *et al.*, Nucl. Instr. and Meth. A **583**, 341 (2007).
[11] I. J. Thompson, Comp. Phys. Rep. **7**, 167 (1988).
[12] K. Hagino, H. Sagawa, J. Carbonell *et al.*, Phys. Rev. Lett. **99**, 022506 (2007).
[13] F. M. Marqués, M. Labiche, N. A. Orr *et al.*, Phys. Rev. C **65**, 044006 (2002).